Biochimica et Biophysica Acta 1863 (2017) 220–230

Contents lists available at ScienceDirect

Biochimica et Biophysica Acta

journal homepage: www.elsevier.com/locate/bbadis

The matrikine N-acetylated proline-glycine-proline induces premature senescence of nucleus pulposus cells via CXCR1-dependent ROS accumulation and DNA damage and reinforces the destructive effect of these cells on homeostasis of intervertebral discs

Chencheng Feng [1], Yang Zhang [1], Minghui Yang [1], Minghong Lan [1], Huan Liu [1], Jian Wang [1], Yue Zhou *[,1], Bo Huang *[,1]

Department of Orthopedics, Xinqiao Hospital, Third Military Medical University, Chongqing 400037, People's Republic of China

ARTICLE INFO

Article history:
Received 3 July 2016
Received in revised form 15 September 2016
Accepted 16 October 2016
Available online 19 October 2016

Keywords:
Matrikine
N-acetylated proline-glycine-proline
Disc cell senescence
Cellular antioxidant system
Homeostasis of intervertebral disc
Intervertebral disc degeneration

ABSTRACT

Intervertebral disc (IVD) cell senescence is a recognized mechanism of intervertebral disc degeneration (IDD). Elucidating the molecular mechanisms underlying disc cell senescence will contribute to understanding the pathogenesis of IDD. We previously reported that N-acetylated proline-glycine-proline (N-Ac-PGP), a matrikine, is involved in the process of IDD. However, its roles in IDD are not well understood. Here, using rat nucleus pulposus (NP) cells, we found that N-Ac-PGP induced premature senescence of NP cells by binding to CXCR1. N-Ac-PGP induced DNA damage and reactive oxygen species accumulation in NP cells, which resulted in activation of the p53-p21-Rb and p16-Rb pathways. Moreover, the RT^2 profiler PCR array showed that N-Ac-PGP down-regulates the expression of antioxidant genes in NP cells, suggesting a decline in the antioxidants of NP cells. On the other hand, N-Ac-PGP up-regulated the expression of matrix catabolic genes and inflammatory genes in NP cells. Concomitantly, N-Ac-PGP reinforced the destructive effects of senescent NP cells on the homeostasis of the IVDs in vivo. Our study suggests that N-Ac-PGP plays critical roles in the pathogenesis of IDD through the induction of premature senescence of disc cells and via the activation of catabolic and inflammatory cascades in disc cells. N-Ac-PGP also deteriorates the redox environment of disc cells. Hence, N-Ac-PGP is a new potential therapeutic target for IDD.

1. Introduction

Intervertebral disc (IVD) cell senescence is a newly recognized hallmark of intervertebral disc degeneration (IDD) [1,2]. Cell senescence is an irreversible growth-arrested state. Various intrinsic and extrinsic triggers, such as telomere erosion, oxidative stress, DNA damage, abnormal mechanical loading and pro-inflammatory cytokines, activate the p53–p21-retinoblastoma protein (Rb) and p16-Rb signaling pathways to arrest the cell-cycle progression of IVD cells [3–5]. Senescent disc cells are replication exhausted. As a result, the number of functional cells in the IVD decreases due to apoptosis or cell death. In addition to replicative exhaustion, the senescence-associated secretory phenotype (SASP) of senescent disc cells is characterized by aberrant production of extracellular matrix (ECM) proteases, chemokines and cytokines [6,7]. These secreted proteins enhance ECM catabolism and inflammation in the microenvironment of discs, suggesting that disc cell senescence makes a critical contribution to the pathogenesis of IDD [8,9]. Therefore, elucidating the mechanisms underlying disc cell senescence will contribute to better understanding the pathogenesis of IDD.

Abbreviations: IVD, intervertebral disc; IDD, intervertebral disc degeneration; SASP, senescence-associated secreted phenotype; NP, nucleus pulposus; AF, annulus fibrosus; SA-β-Gal, senescence-associated β-galactosidase; ECM, extracellular matrix; DDR, DNA damage response; N-Ac-PGP, N-acetylated proline-glycine-proline; RS, replicative senescence; Rb, retinoblastoma protein; RPX, Reparixin; ADAMTS, a disintegrin and metalloproteinase with thrombospondin motifs; MMP, matrix metalloproteinase; PE, prolyl endopeptidase; p-Rb, phosphorylated retinoblastoma protein; ROS, reactive oxygen species; FBS, fetal bovine serum; P, passage; PBS, phosphate-buffered saline; PD, population doubling; Txnrd, thioredoxin reductase; Gsr, glutathione reductase; Gpx, glutathione peroxidase; Prdx, peroxiredoxin; Vimp, VCP interacting membrane selenoprotein; Nudt1, nudix hydrolase 1; Nqo1, NAD(P)H quinone dehydrogenase 1; Epx, eosinophil peroxidase; Apoe, apolipoprotein E; GSH, glutathione; Trx, thioredoxin.

* Corresponding authors.
E-mail addresses: doctorfgy@163.com (C. Feng), 65210796@qq.com (Y. Zhang), doc_ymh@163.com (M. Yang), fccdoc@me.com (M. Lan), 20016040@163.com (H. Liu), tonywjxq@aliyun.com (J. Wang), happyzhou@vip.163.com (Y. Zhou), fmmuhb@126.com (B. Huang).
[1] Xinqiao Main Street 183, Shapingba District Chongqing, People's Republic of China.

http://dx.doi.org/10.1016/j.bbadis.2016.10.011

The ECM-derived matrikines reinforce inflammation in the tissue microenvironment [10,11]. The matrikine N-acetylated proline-glycine-proline (N-Ac-PGP) is generated from collagen via the activity of sequential proteases (matrix metalloproteinase (MMP) 8, MMP9 and prolyl endopeptidase (PE)) [12]. It is a ligand of CXCR1/2 and a neutrophil chemokine. It is involved in many inflammatory diseases, including chronic obstructive pulmonary disease, inflammatory bowel diseases and ischemic stroke [13–15]. We recently found that the levels of N-Ac-PGP in human nucleus pulposus (NP) tissues are positively correlated with the degree of disc degeneration [16], suggesting that N-Ac-PGP is involved in the establishment and progression of IDD. Nevertheless, the precise roles of N-Ac-PGP in the pathogenesis of IDD remain unclear. Interestingly, CXCR1/2 have been shown to reinforce cell senescence [17,18]. Thus, in the IVD microenvironment, where N-Ac-PGP is present, N-Ac-PGP likely contributes to the progression of IDD by regulating disc cell senescence. However, there have been no studies on the relationship between N-Ac-PGP and disc cell senescence reported to date.

In the present study, we established an in vitro replicative senescence (RS) model using rat NP cells through serial culturing. These NP cells were then treated with N-Ac-PGP during continuous passaging. Growth, senescence-associated β-galactosidase (SA-β-gal) staining and senescence-related molecular pathways were examined at different passages to investigate the roles of N-Ac-PGP in NP cell senescence. The RT^2 Profiler PCR Array was used to investigate the oxidative stress in N-Ac-PGP-treated cells. We also examined the effects of N-Ac-PGP on the SASP of NP cells. Finally, the influence of senescent NP cells on the structure and function of the IVD was evaluated through in vivo assays. The detrimental effects of these cells were enhanced by N-Ac-PGP. This study provides a novel insight into the causes and molecular mechanisms of disc cell senescence. Regulating N-Ac-PGP may retard disc cell senescence, and N-Ac-PGP represents a new potential therapeutic target for IDD.

2. Materials and methods

2.1. Ethics statement

This study has been conducted in accordance with the ethical standards set by the Declaration of Helsinki. It has been approved by the Ethical Committee of Xinqiao Hospital. It met the NIH guidelines for the care and use of laboratory animals.

2.2. Reagents

N-Ac-PGP was purchased from Sigma-Aldrich (Sigma, St. Louis, MO, USA). Reparixin and AB89251 were provided by MedChemexpress (Princeton, NJ, USA) and Abcam (Cambridge, MA, USA), respectively. Mouse antibodies against GAPDH, BrdU, p53, p21, p16, phosphorylated-Rb (p-Rb), CXCR1 and CXCR2 as well as rabbit antibodies against Rb, MMP13 and a disintegrin and metalloproteinase with thrombospondin motifs 5 (ADAMTS5) were purchased from Santa Cruz Biotechnology (Santa Cruz, CA, USA). The mouse antibody against histone γ-H2A.X was purchased from Cell Signaling Technology (Danvers, MA, USA). Relevant HRP-conjugated, Alexa Fluor 488 dye-conjugated and Alexa Fluor 647 dye-conjugated secondary antibodies were purchased from Thermo Scientific (Waltham, MA, USA).

2.3. Isolation and culture of rat NP cells

Caudal IVDs (C1-C10) were harvested from adult (12-week-old) male Sprague Dawley rats (Laboratory Animal Research Center of Daping Hospital, Chongqing, China) that were sacrificed via excessive pentobarbital. The translucent and gelatinous NP tissues were squeezed out from the incision of AF caused by a straight sharp-pointed scalpel, and then, were digested in DMEM/F12 medium (Invitrogen, Carlsbad, CA, USA) containing 0.2% type II collagenase (Sigma, St. Louis, MO, USA) at 37 °C for 4 h. After being passed through a 70 μm cell strainer, the cell suspension was centrifuged at 1000 rpm for 5 min. Then, the supernatant was removed, and the cell pellet was resuspended in DMEM/F12 medium containing 10% fetal bovine serum (FBS) and 1% penicillin-streptomycin (Invitrogen, Carlsbad, CA, USA). The isolated NP cells were subsequently cultured at 37 °C and 5% CO_2, which was defined as passage 0 (P0). The medium was replaced twice a week. When confluent, the cells were subcultured, and their culture passage number increased by one. Serial culturing was performed to establish the RS model of NP cells. In order to determine the lifespan of NP cells, starting from P0, NP cells were seeded at a density of $4 \times 10^3/cm^2$ in 25 cm^2 culture flasks. After 7 days of culture, the cells were trypsinized, counted and reseeded at $4 \times 10^3/cm^2$ in 25 cm^2 culture flasks. The population doubling (PD) of each period of seven days was calculated using the following equation: $PD = [\log10(NH) - \log10(NI)] / \log10(2)$, where NH is the number of cells at the end of seven days, and NI is the initial number of seeded cells. An increase in the PD was added to the previous PD to calculate cumulative PD. The in vitro lifespan of NP cells was determined based on the cumulative PD. It was 35–36 cumulative PD (data not shown). In our study, the culture days of NP cells at P6 were 60–70 days, and the cumulative PD of these cells was 33–34. Thus, NP cells at P6 were regarded as the cells with replicative senescence because they were close to their Hayflick limit.

2.4. N-Ac-PGP treatment during serial replication

When the cells were subcultured from P0 to P1, culture medium containing N-Ac-PGP (100 ng/ml) was used. This concentration was found to up-regulate the expression of p21 and p16 in NP cells without cytotoxicity in preliminary experiments (data not shown). Cells at different passages were used in subsequent experiments. NP cells that were not subjected to N-Ac-PGP treatment served as a control. For CXCR1 inhibition, the cells were treated with Reparixin (RPX, 1 μg/ml) and AB89251 (AB, 100 ng/ml) for 30 min before the culture medium was changed to DMEM/F12 containing N-Ac-PGP and RPX or AB.

2.5. SA-β-gal staining

SA-β-gal staining was performed using an SA-β-gal staining kit (Cell Signaling Technology, Danvers, MA, USA) according to the manufacturer's protocol. Briefly, cells seeded in 12-well plates (1×10^3 cells per well) were washed using phosphate-buffered saline (PBS) and fixed with 2% formaldehyde for 20 min at room temperature. After being washed with PBS, the cells were incubated with the staining solution containing X-gel (1 mg/ml) at 37 °C for 12 h. Then, the percentage of SA-β-gal-positive cells in nine random fields was determined using a phase-contrast microscope (200×, Olympus, Tokyo, Japan), and the mean percentage was calculated.

2.6. Cell growth assay

The growth of NP cells was assessed using Cell Counting Kit-8 Assay (CCK-8, Dojindo, Tokyo, Japan). The cells were seeded in 96-well plates, then incubated with 10 μl of CCK-8 reagent for 2 h at 37 °C, and the absorbance was measured at 450 nm using a spectrophotometer (Varioskan Flash, Thermo Scientific, Waltham, MA, USA). The number of cells was calculated based on the absorbance according to the standard curve. The assay was performed once a day on seven consecutive days. The population doubling (PD) was calculated every day using the following equation [19]: $PD = [\log10(NH) - \log10(NI)] / \log10(2)$, where NH is the number of cells at each time point, and NI is the initial number of seeded cells. The growth curve of NP cells was depicted based on the PD value.

2.7. Telomerase activity

Telomerase activity was evaluated using a TRAPeze® RT Telomerase Detection Kit (Millipore Billerica, MA, USA). Briefly, NP cells were resuspended in 200 μl of CHAPS Lysis Buffer/10^5–10^6 cells. After incubation on ice for 30 min, the sample was centrifuged at 12,000 ×*g* for 20 min at 4 °C. The protein concentration was diluted to 750 ng/μl. One aliquot of each sample was incubated at 85 °C for 10 min to serve as the heat-treated negative control, and the positive control, minus control and no template control were prepared based on the manufacturer's instructions. A 25 μl reaction volume was employed for PCR amplification. The reactions were run under the following conditions: 30 °C for 30 min, then 95 °C for 2 min, followed by 45 cycles of 94 °C for 5 s, 59 °C for 60 s and 45 °C for 10 s. The average cycle threshold (Ct) measurement for each sample was used to quantitate telomerase activity based on the TSR8 standard curve generated according to the manufacturer's protocol.

2.8. Reactive oxygen species (ROS) measurement

The levels of ROS in NP cells were measured using the H2DCF-DA assay (Sigma, St. Louis, MO, USA). NP cells were incubated with 25 μM H2DCF-DA in PBS under 5% CO_2 for 30 min at 37 °C. The mean fluorescence intensity was measured with a flow cytometer (Beckman, CA, USA).

2.9. BrdU incorporation assay and immunofluorescence assay

For BrdU incorporation assay, NP cells were incubated with BrdU (1 μg/ml) under 5% CO_2 for 12 h at 37 °C, and then were fixed with 70% of ethanol. After wash with PBS, cells were treated with 2 mol/l HCl at room temperature for 30 min. For immunofluorescence assay, NP cells plated in culture dishes were washed using PBS, followed by fixation with 4% paraformaldehyde for 30 min. After being permeabilized and subjected to antigen blocking, cells were incubated with primary antibodies against γ-H2A.X (1:400 dilution), BrdU (1:50 dilution), CXCR1 (1:200 dilution) and CXCR2 (1:50 dilution) overnight at 4 °C. After rinsing, the cells were incubated with respective secondary antibodies in the dark and then stained with DAPI (0.1 mg/ml, Sigma, St. Louis, MO, USA). Cells that were not incubated with the primary antibodies served as the negative control. Images were obtained using a confocal microscope (Lecia, Weltzlar, Germany). The mean percentages of γ-H2AX-positive cells and BrdU-positive cells in six random fields (200×) were calculated.

2.10. RT^2 profiler PCR arrays

NP cell cDNA was synthesized using an RT^2 First Strand Kit (Qiagen, Valencia, CA, USA) according to the manufacturer's protocol. The rat oxidative stress RT^2 profiler PCR array (Qiagen, Valencia, CA, USA), consisting of 84 key genes involved in oxidative stress signaling, was used to analyze the differentially expressed genes between the control and N-Ac-PGP-treated NP cells. Reactions were run on a ViiA™7 Real-time PCR system (Applied Biosystems) under the following condition: 95 °C for 10 min, followed by 45 cycles of 95 °C for 15 s and 60 °C for 1 min. The data were analyzed using PCR array data analysis software at www.SABiosciences.com/pcrarraydataanalysis.php. For each condition, three assays were carried out as independent samples. A fold change ≥2 with a P value ≤ 0.05 were considered to indicate statistical significance.

2.11. Real-time quantitative PCR

Total RNA (1 μg) was employed for reverse transcription using the Primescript RT reagent kit (Takara Bio, Shiga, Japan) according to the manufacturer's protocols. Real-time quantitative PCR was performed in triplicate on a ViiA™7 Real-time PCR system with SYBR® Premix Ex Taq™ II (Takara Bio, Shiga, Japan). The internal reference gene was GAPDH. The 20 μl reaction mixtures were amplified under the following conditions: 95 °C for 30 s, followed by 40 cycles of 95 °C for 5 s and 60 °C for 30 s. The data were analyzed using the $2^{-\Delta\Delta Ct}$ method.

2.12. Western blot analysis

Proteins from NP cells were separated on 10% (*w*/*v*) SDS gels and transferred to PVDF membranes (Millipore Billerica, MA, USA). The membranes were blocked with 5% milk proteins in TBST for 1 h at 37 °C and then incubated with primary antibodies (anti-GAPDH, 1:1000 dilution; anti-p53, 1:700 dilution; anti-p21, 1:500 dilution; anti-Rb, 1:700 dilution; anti-p-Rb, 1:700 dilution; anti-CXCR1, 1:700 dilution; anti-CXCR2, 1:700 dilution; anti-MMP13, 1:500 dilution; anti-ADAMTS5, 1:500 dilution) overnight at 4 °C, followed by incubation with HRP-conjugated secondary antibodies for 1 h at 37 °C. Immunolabeling was detected using ECL reagents (Thermo Scientific, Waltham, MA, USA).

2.13. Delivery of NP cells into the NP of rat caudal discs

Twenty-four six-week-old male SD rats were used. The rats were randomized into six groups. Under intraperitoneal anesthesia with pentobarbital, the skin of tails was incised longitudinally, and then, caudal discs (C5–C9) were exposed by blunt separation. Avoiding excessive damage to spinal muscles was crucial to minimizing the detrimental effects of imbalanced mechanical stress distribution on the structural and functional homeostasis of discs. Untreated cells at P2 or P6 and N-Ac-PGP-treated NP cells at P2 or P6 were resuspended in culture medium without N-Ac-PGP (1×10^3/μl). 20 μl of cell suspension was injected into the C6–7 and C7–8 levels respectively, using a micro-syringe (20 μl). The number of cells injected into each disc was 2×10^4. The needle of the micro-syringe was placed at the center of discs, perpendicular to the caudal spine, parallel to the end plates. The tip of the needle was inserted into discs gradually until the resistance of AF disappeared. Under this condition, the tip was located at the NP of discs. Next, the cell suspension was injected into the NP of discs. The speed of injection should be slow in order to avoid the leaking out of the cell suspension. For the sham-operated control rats, 20 μl of culture medium without N-Ac-PGP and NP cells was injected into the C6–7 and C7–8 discs. Discs at the same level in rats not subjected to operation served as the blank control, while untreated C5–6 and C8–9 discs served as the internal control. The rats were fed normally and monitored. At the first week and second week after the operation, MRI of the rats' caudal spines was performed. Finally, the rats were sacrificed, and the relevant IVDs were collected for histological analyses.

2.14. MRI processing

MRI was performed to evaluate the T2-weighted signal of the NP and the structural changes in the caudal discs using a 3.0 T MRI system (GE, Fairfield, Conn, USA). Five serial sagittal T2-weighted sections were obtained using the following settings: time to repetition of 300 ms, time to echo of 15 ms, and a 2 mm slice thickness. The grades of disc degeneration were defined [20]. The T2 intensity and the area of the NP were measured using Osirix Lite software. All images were evaluated and measured by two spine surgeons in a blinded fashion to the treatment of injected cells and follow-up time. Each observer reevaluated all images at one week after first evaluation. The intraobserver and interobserver reliabilities of the evaluations and measurements were determined using kappa statistics [21].

2.15. Histological analysis

Fixed rat caudal discs were embedded in paraffin and sectioned sagittally at a thickness of 2 μm. The sections were stained with hematoxylin and eosin (H&E). Images were obtained with an Olympus BX60 microscope (Olympus, Tokyo, Japan). The grade of histological degeneration was evaluated based on grading scales described in previous studies [21] (Table 1). All histological sections were graded by two observers in a blinded fashion using random labeled slides, and were reevaluated at one week after first evaluation. As also, the interobserver and intraobserver reliabilities were determined using kappa statistics.

2.16. Statistical analysis

All measurements were performed on at least three replicates. The data are shown as the means or means ± SEM. For comparisons between two independent samples, a two-tailed Student's *t*-test was used. For comparisons between three or more groups, one-way ANOVA and least-significant difference (LSD) multiple comparisons were employed. The data for the quantitative PCR assays, the Pfirrmann scores and the histological grades of IVDs were statistically tested using Kruskal-Wallis nonparametric analysis and Mann-Whitney U post-hoc tests as described previously [21,22]. The data were analyzed with the GraphPad Prism 6 and SPSS version 22.0 software programs. $P < 0.05$ was considered to indicate statistical significance.

3. Results

3.1. RS of rat NP cells

NP cells were cultured serially to establish the RS model. The growth of NP cells arrested with increasing passages, which was accompanied by decreased incorporation of BrdU (Fig. 1A, C, E). Additionally, the percentage of SA-β-gel-positive cells increased as the morphology of NP cells became larger and flatter (with advancing passages; Fig. 1B, D). The results demonstrate the RS of NP cells during serial replication.

With regard to the triggers and molecular mechanisms underlying the RS of NP cells, a gradual decline in telomerase activity and an increase in the percentage of γ-H2A.X-positive cells (DNA damage marker) were observed with increasing passages (Fig. 1F, G, H). Consequently, the expression of p53 and p21 in NP cells was up-regulated (Fig. 1J, K). In addition, the levels of ROS in the cells at later passages were significantly higher than those in early passages, significantly up-regulating p16 in NP cells (Fig. 1I, J, K). The expression of p-Rb was low in NP cells, regardless of the number of passages. However, the expression of Rb was up-regulated in NP cells with serial replication, suggesting that hypo-phosphorylation of Rb in the senescent NP cells (Fig. 1J, K).

3.2. N-Ac-PGP induced premature senescence of NP cells through CXCR1

To investigate the roles of N-Ac-PGP in NP cell senescence, rat NP cells were cultured using medium containing N-Ac-PGP. This N-Ac-PGP exposure led to a prominent suppression of the growth of NP cells and the incorporation of BrdU in NP cells at P2 (Fig. 2A, B, D). However, this effect was gradually attenuated with increasing passage numbers (Supplementary Fig. S1A, B). Furthermore, compared with the control, the N-Ac-PGP-treated NP cells showed more SA-β-gel-positive cells at P2 (Fig. 2C, Supplementary Fig. S2). This difference was also gradually eliminated with increasing passage number (Supplementary Fig. S1C).

To test whether CXCR1/2 mediates the pro-senescence effect of N-Ac-PGP on NP cells, the expression of CXCR1/2 in NP cells was investigated. Interestingly, rat NP cells expressed CXCR1 rather than CXCR2 (Supplementary Fig. S3A, B). Therefore, a CXCR1 inhibitor (RPX) and an antibody that neutralizes CXCR1 (AB) were used for inhibition assays. The premature senescence of NP cells induced by N-Ac-PGP was significantly retarded in the presence of RPX and AB (Fig. 2, Supplementary Fig. S2).

3.3. N-Ac-PGP enhanced DNA damage in NP cells and activated the p53-p21-Rb pathway via CXCR1

N-Ac-PGP did not affect telomerase activity in NP cells (Fig. 3F). However, N-Ac-PGP exposure increased the percentage of γ-H2A.X-positive NP cells (Fig. 3A, B), suggesting that there was an increase in DNA damage induced by N-Ac-PGP. Accordingly, the expression of p53, p21 and Rb in NP cells was up-regulated by N-Ac-PGP (Fig. 3D, E). However, the expression of p-Rb did not show any significant changes in the N-Ac-PGP-treated cells. Antagonizing CXCR1 inhibited the N-Ac-PGP-induced DNA damage as well as the activation of the p53-p21-Rb pathway in NP cells (Fig. 3A, B, D, E).

3.4. N-Ac-PGP promoted ROS production and up-regulated the expression of p16 in NP cells via CXCR1

The levels of ROS and the expression of p16 in NP cells were significantly increased by N-Ac-PGP, which was suppressed by antagonizing CXCR1 (Fig. 3C, D, E). The RT^2 profiler PCR array was used to investigate the expression of oxidative stress genes and antioxidant-related genes in NP cells. Eleven genes were differentially expressed. Antioxidant-related genes in NP cells were significantly down-regulated by N-Ac-PGP, including thioredoxin reductase (Txnrd) 1 (Txnrd1), Txnrd2, glutathione peroxidase (Gpx) 1, Gpx3, glutathione reductase (Gsr) and peroxiredoxin 6 (Prdx6). On the other hand, oxidative stress response genes, such as VCP interacting membrane selenoprotein, nudix hydrolase 1, NAD(P)H quinone dehydrogenase 1, and eosinophil peroxidase and apolipoprotein E were significantly up-regulated by N-Ac-PGP (Table 2).

3.5. The SASP of replicatively senescent NP cells

The proteins related to the SASP are regulated at the mRNA level [23]. Fig. 4A shows the up-regulation of major ECM proteases (MMP2, MMP13, ADAMTS4, ADAMTS5) in NP cells at P6 compared with NP cells at P2. MMP13 and ADAMTS5 were selected as representative proteases for further investigation through western blot analysis. The results were consistent with those of the PCR analysis (Fig. 4C). On the other hand, the expression levels of several inflammatory factors, including IL-6, CCL5, CXCL10 and CCL2, were slightly up-regulated in NP

Table 1
Histological degeneration grading scores of intervertebral discs.

Scores	Nucleus pulposus (NP)	Annulus fibrosus (AF)
0	Normal cellularity, large vacuolated cells, stellar-shaped cell nucleus, and consistent cell distribution	Well-organized AF without rupture or serpentine fibers
1	Decrease in the number of cells (<50%) regardless of cell clustering	AF with rupture or serpentine fibers (<30%)
2	Decrease in the number of cells (>50%), few vacuolated cells, occupation by proliferative connective tissue (<50% of NP area)	AF with rupture, serpentine fibers (>30%) or reversed outline
3	Occupation by proliferative connective tissue (>50% of NP area), small area of vacuolated cells	Indistinguishable and disorganized AF

Scores range from a normal intervertebral disc (0) to severely degenerative disc (6).

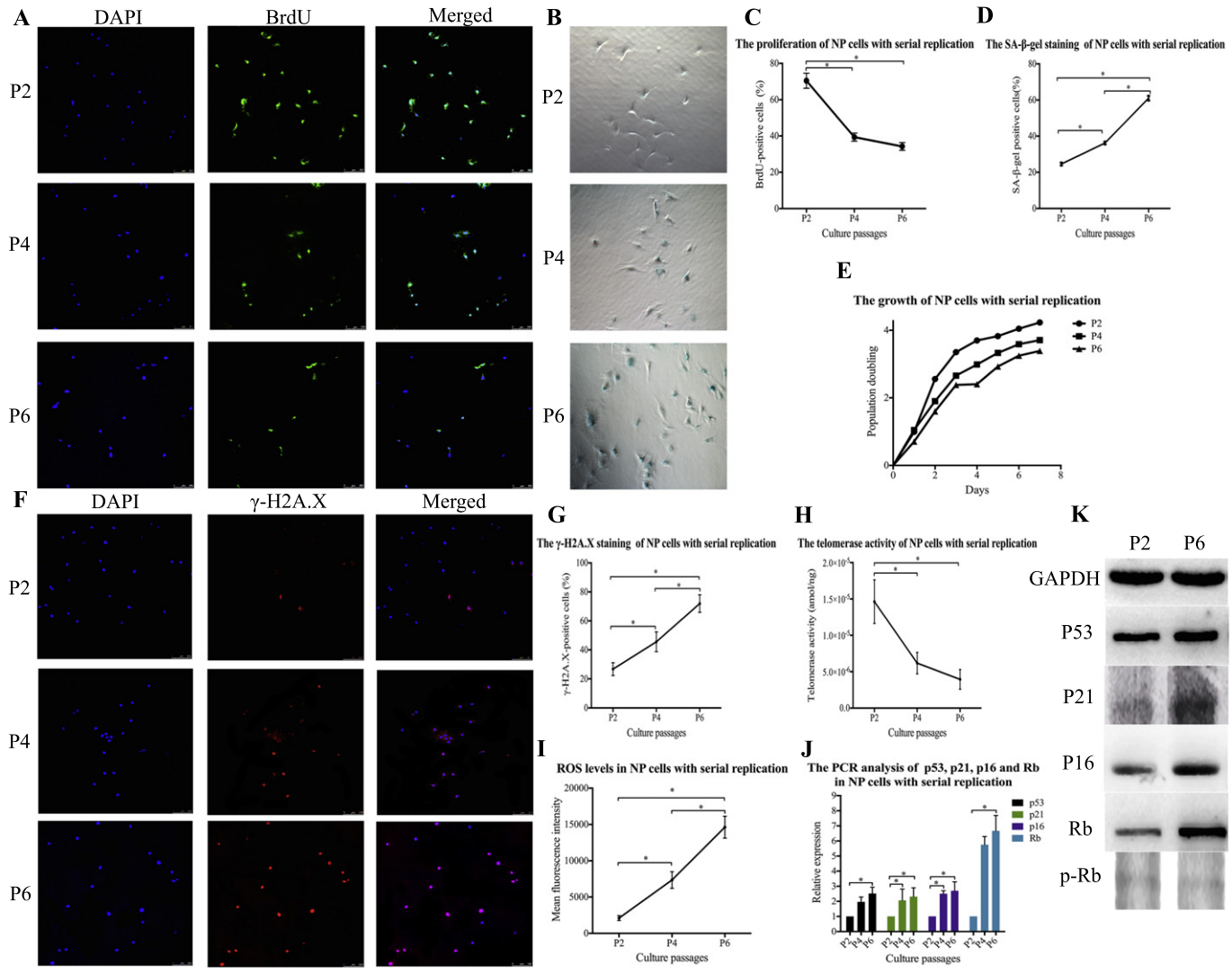

Fig. 1. The replicative senescence of rat nucleus pulposus (NP) cells. (A, C) Immunofluorescence staining of BrdU and the percentage of BrdU-positive cells in NP cells at different passages (B, D) Senescence-associated β-galactosidase (SA-β-gal) staining and the percentage of SA-β-gal-positive cells in NP cells at different passages. (E) The growth of NP cells at different passages. (F, G) Immunofluorescence staining of γ-H2A.X and the percentage of γ-H2A.X-positive cells in NP cells at different passages. (H) The telomerase activity in NP cells at different passages. (I) The production of ROS in NP cells at different passages. (J, K) The quantitative PCR analysis and western blot analysis of p53, p16, p21, retinoblastoma protein (Rb) and phosphorylated Rb (p-Rb) in NP cells. *, P value < 0.05, error bars represent standard error. Abbreviations: P2, passage 2; P4, passage 4; P6, passage 6.

cells at P6 (Fig. 4B). In summary, in the RS model employing NP cells, the SASP was characterized by a catabolic and inflammatory phenotype.

3.6. Effects of N-Ac-PGP on the SASP of NP cells

N-Ac-PGP significantly up-regulated the expression of MMP2, MMP3, MMP13, ADAMTS4 and ADAMTS5 in NP cells at P2. This up-regulation of most of these ECM proteases induced by N-Ac-PGP was suppressed by CXCR1 inhibition, although there was no effect on MMP3 (Fig. 4D). The expression of MMP13 and ADAMTS5 was validated through western blot analysis (Fig. 4F). In NP cells at P6, the up-regulation of ECM proteases induced by N-Ac-PGP was attenuated (Fig. 4E). On the contrary, the expression of most inflammatory factors was not significantly up-regulated by N-Ac-PGP in NP cells at P2 (with the sole exception of CCL2; Fig. 4G). However, N-Ac-PGP significantly increased the expression of IL-6, CCL2, CCL5 and CXCL10 in NP cells at P6, which was also prevented by CXCR1 inhibition (Fig. 4H). Although the influence of N-Ac-PGP on the SASP of NP cells was passage-dependent, in general, N-Ac-PGP reinforced the catabolic and inflammatory cascades in NP cells.

3.7. N-Ac-PGP reinforced the destructive effects of senescent NP cells on rat IVDs

To investigate the cause-effect relationship between disc cell senescence and IDD, we delivered senescent NP cells into rat caudal IVDs, and the structure of the discs was subsequently evaluated via MRI. In the blank control group, C6–7 and C7–8 levels showed minimal changes in T2 intensity and structure at both time points (week 1 and week 2) compared with C5–6 and C8–9 (Fig. 5A). Additionally, there were no degenerative changes in the sham-operated discs. However, the C6–7 and C7–8 levels injected with untreated cells at P6 or N-Ac-PGP-treated cells at P6 showed slight degeneration at one week after operation, including a decreased T2 intensity and a shrunken NP area. At week 2, these signs of degeneration were dramatically increased (Fig. 5A, B, C). The Pfirrmann scores of the discs injected with N-Ac-PGP-treated cells at P6 or untreated cells at P6 increased from week 1

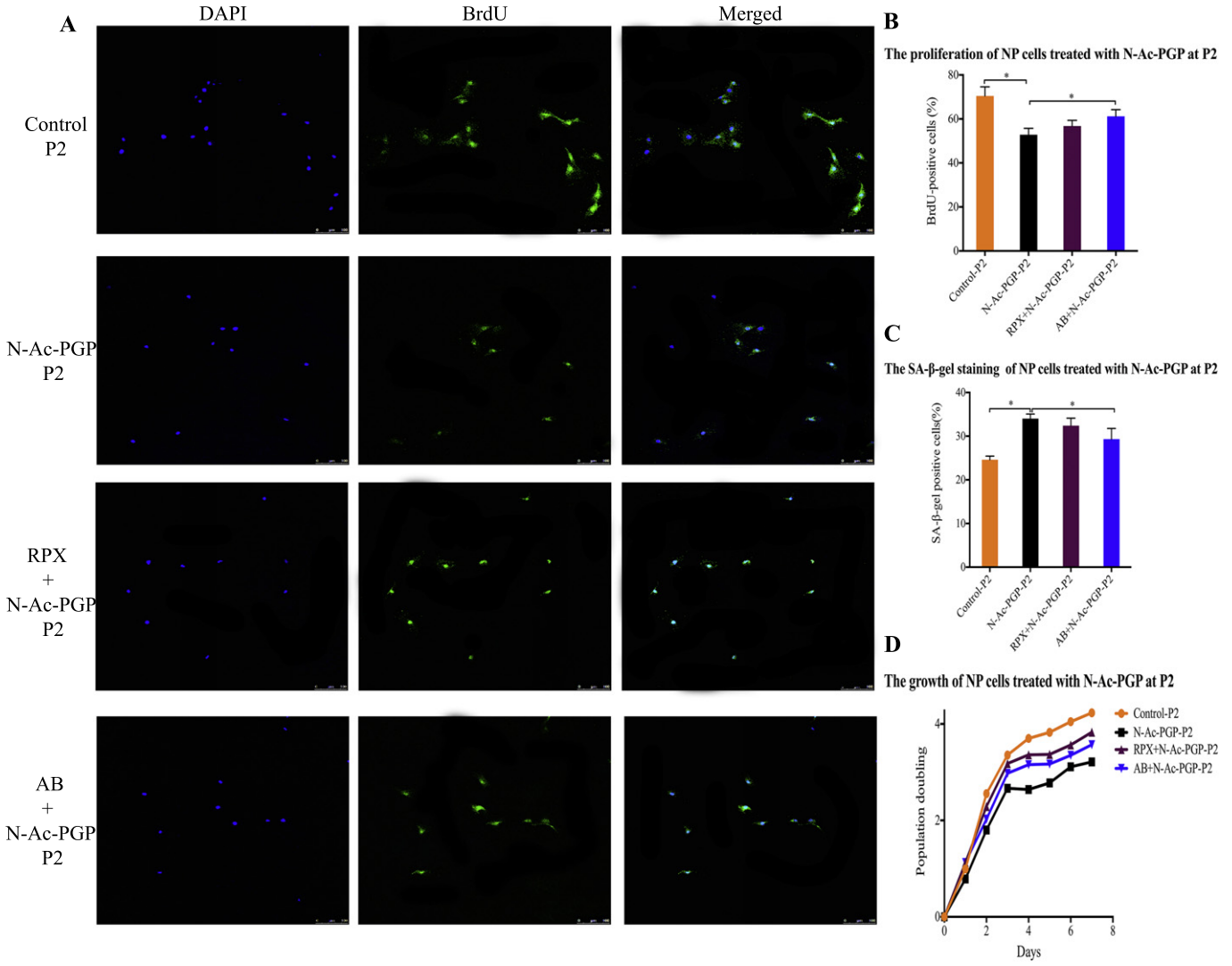

Fig. 2. The premature senescence of nucleus pulposus (NP) cells induced by N-acetylated proline-glycine-proline (N-Ac-PGP). (A, B) Immunofluorescence staining of BrdU and the percentage of BrdU-positive cells in N-Ac-PGP-treated NP cells at passage 2 (P2). (C) The percentage of senescence-associated β-galactosidase (SA-β-gal)-positive cells in N-Ac-PGP-treated NP cells at P2. (D) The growth of N-Ac-PGP-treated NP cells at P2. The cells without N-Ac-PGP treatment served as the control. The cells were pretreated with the RPX and AB for 30 min followed by N-Ac-PGP treatment for CXCR1 inhibition. *, P value < 0.05, error bars represent standard error. Abbreviations: RPX, Reparixin; AB, AB89251.

to week 2. More importantly, the heights of the discs injected with N-Ac-PGP-treated cells at P6 collapsed, leading to higher Pfirrmann scores than those injected with untreated cells at P6 (Fig. 5A, D). Notably, the discs injected with untreated cells at P2 and N-Ac-PGP-treated cells at P2 showed few degenerative changes (Fig. 5A).

Microscopically, the discs in the blank control group showed well-organized lamellae in the annulus fibrosus (AF) and normal cellularity with large vacuolized cells in the NP. The sham-operated discs and the discs injected with untreated cells or N-Ac-PGP-treated cells at P2 did not show any obvious structural changes (Fig. 6, Supplementary Figs. S4, S5). However, at week 1, the NP cellularity of the discs injected with untreated cells or N-Ac-PGP-treated cells at P6 was decreased (Supplementary Fig. S4). At week 2, the NP area of the discs injected with untreated cells at P6 decreased dramatically and was replaced by proliferative connective tissues. The AF became disorganized, with ruptured and reversed serpentine fibers. The discs injected with N-Ac-PGP-treated cells at P6 showed more severe degenerative changes, with the NP being completely replaced by proliferative connective tissues (Fig. 6). The structural changes in IVDs were evaluated using a histological grading system (Table 1). The histological scores of the discs injected with N-Ac-PGP-treated cells or untreated cells at P6 increased from week 1 to week 2. The scores of the discs injected with N-Ac-PGP-treated cells at P6 were significantly higher than those of the discs injected with untreated cells at P6 (Fig. 5E).

4. Discussion

In this study, N-Ac-PGP was found to induce premature senescence and enhance matrix catabolism and inflammatory cascades of NP cells. Moreover, intradiscal delivery of senescent NP cells into rat caudal IVDs accelerated the process of IDD. N-Ac-PGP exaggerated the detrimental effects of senescent NP cells on the homeostasis of the IVD.

Culturing NP cells serially in vitro has been demonstrated to provide a reasonable model for investigating the RS of NP cells [24]. Herein, the RS of rat NP cells occurred due to declined telomerase activity, ROS accumulation and DNA damage. Both the p53-p21-Rb and p16-Rb pathways were activated. These findings are consistent with previous studies based on human NP cells [3]. It suggests that intrinsic triggers, such as DNA damage and oxidative stress, accumulate with NP cell aging to induce cell senescence. Both the p53-p21-Rb and p16-Rb pathways play central roles in halting cell-cycle progression in NP cells.

Numerous extrinsic stimuli in the microenvironment of degenerative discs have been reported to regulate disc cell senescence, including pro-inflammatory cytokines, growth factors, glucose and mechanical

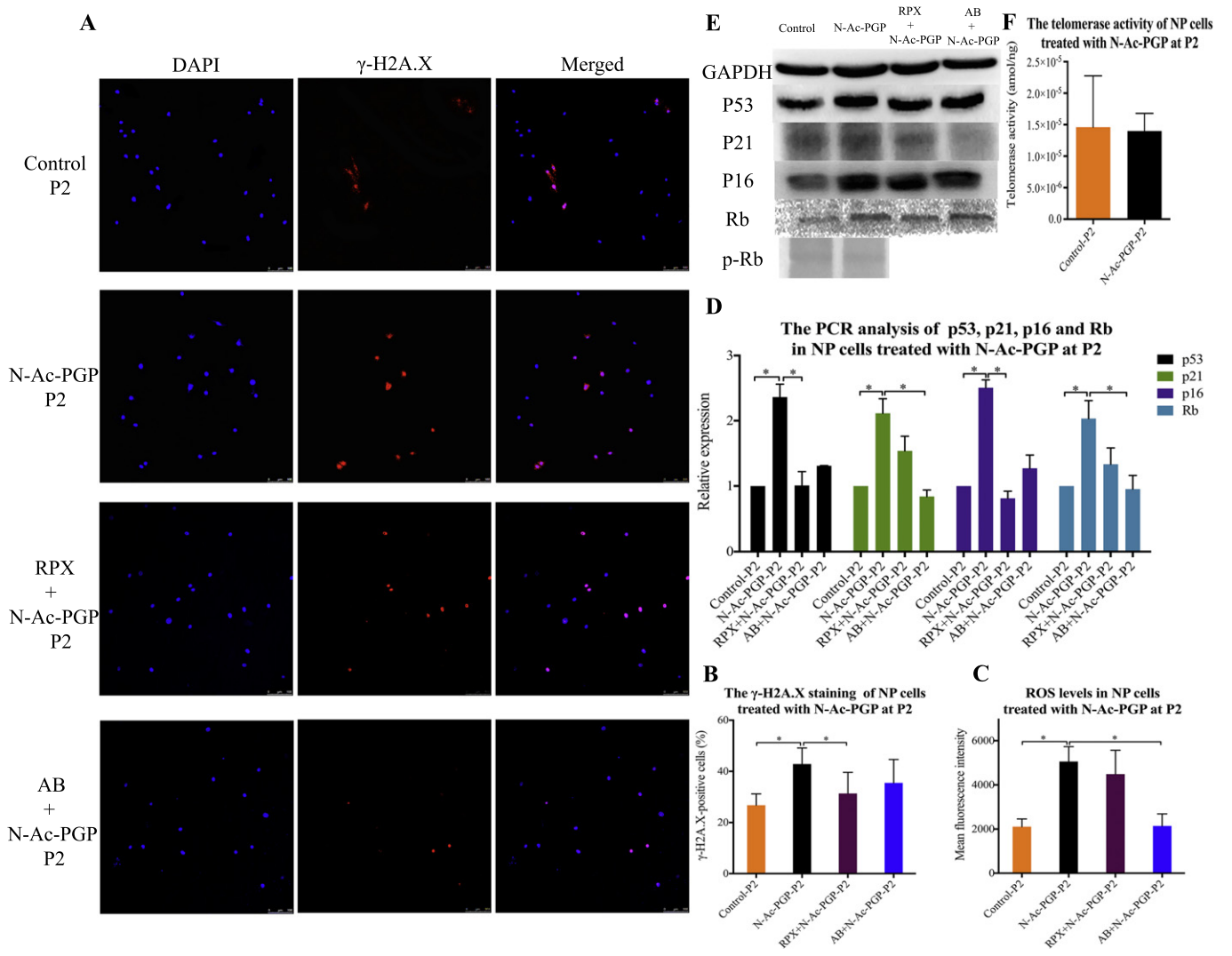

Fig. 3. The molecular mechanism of premature senescence of nucleus pulposus (NP) cells induced by N-acetylated proline-glycine-proline (N-Ac-PGP) (A, B) Immunofluorescence staining of γ-H2A.X and the percentage of γ-H2A.X-positive cells in N-Ac-PGP-treated NP cells at passage 2 (P2). (C) The production of ROS in N-Ac-PGP-treated NP cells at P2. (D, E) The quantitative PCR analysis and western blot analysis of p53, p16, p21, retinoblastoma protein (Rb) and phosphorylated Rb (p-Rb) in N-Ac-PGP-treated NP cells at P2. (F) The telomerase activity in N-Ac-PGP-treated NP cells at P2. The cells without N-Ac-PGP treatment served as the control. The cells were pretreated with the RPX and AB for 30 min followed by N-Ac-PGP treatment for CXCR1 inhibition. *, P value < 0.05, error bars represent standard error. Abbreviations: RPX, Reparixin; AB, AB89251.

loading [25]. We have identified a positive correlation between the levels of N-Ac-PGP in NP tissues and the Pfirrmann scores of IVDs. N-Ac-PGP is a potent chemokine and pro-inflammatory matrikine in IVDs [16]. However, the roles of N-Ac-PGP in disc cell senescence have remained unclear. Here, we determined that N-Ac-PGP play a critical role in IDD via the induction of premature senescence of NP cells and through the expression of catabolic and inflammatory genes in NP cells. To our knowledge, this is the first study to identify the association

Table 2
Differentially expressed oxidative stress-related genes induced by N-acetylated proline-glycine-proline.

Gene name	Fold regulation	P value	Gene description
Vimp	+2.87	0.038	Oxidative stress response gene, selenoprotein
Nudt1	+5.39	0.037	Oxidative stress response gene, enzyme to degrade 8-oxoguanine-containing deoxyribonucleoside triphosphate
Epx	+3.33	0.025	Oxidative stress response gene, a member of the peroxidase gene family and is expressed in eosinophils
Nqo1	+4.6	0.024	Oxidative stress response gene, enzyme to reduce quinones to hydroquinones
Apoe	+2.87	0.031	Oxidative stress response gene, encode a tumor suppressor protein
Txnrd1	−2.89	0.018	Antioxidant gene, enzyme to reduce thioredoxins
Txnrd2	−2.65	0.048	Antioxidant gene, enzyme to reduce thioredoxins
Gpx1	−3.56	0.012	Antioxidant gene, a member of the glutathione peroxidase family
Gpx3	−3.86	0.016	Antioxidant gene, a member of the glutathione peroxidase family
Gsr	−2.51	0.028	Antioxidant gene, enzyme to reduce oxidized glutathione disulfide
Prdx6	−4.23	0.034	Antioxidant gene, enzyme to catalyze the catabolism of hydrogen peroxide

Abbreviation: +: up-regulation; −: down-regulation; Vimp: VCP interacting membrane selenoprotein; Nudt1: nudix hydrolase 1; Nqo1: NAD(P)H quinone dehydrogenase 1; Epx: eosinophil peroxidase; Apoe: apolipoprotein E; Txnrd1: thioredoxin reductase 1; Txnrd2: thioredoxin reductase 2; Gpx1: glutathione peroxidase 1; Gpx3: glutathione peroxidase 3; Gsr: glutathione reductase; Prdx6: peroxiredoxin 6.

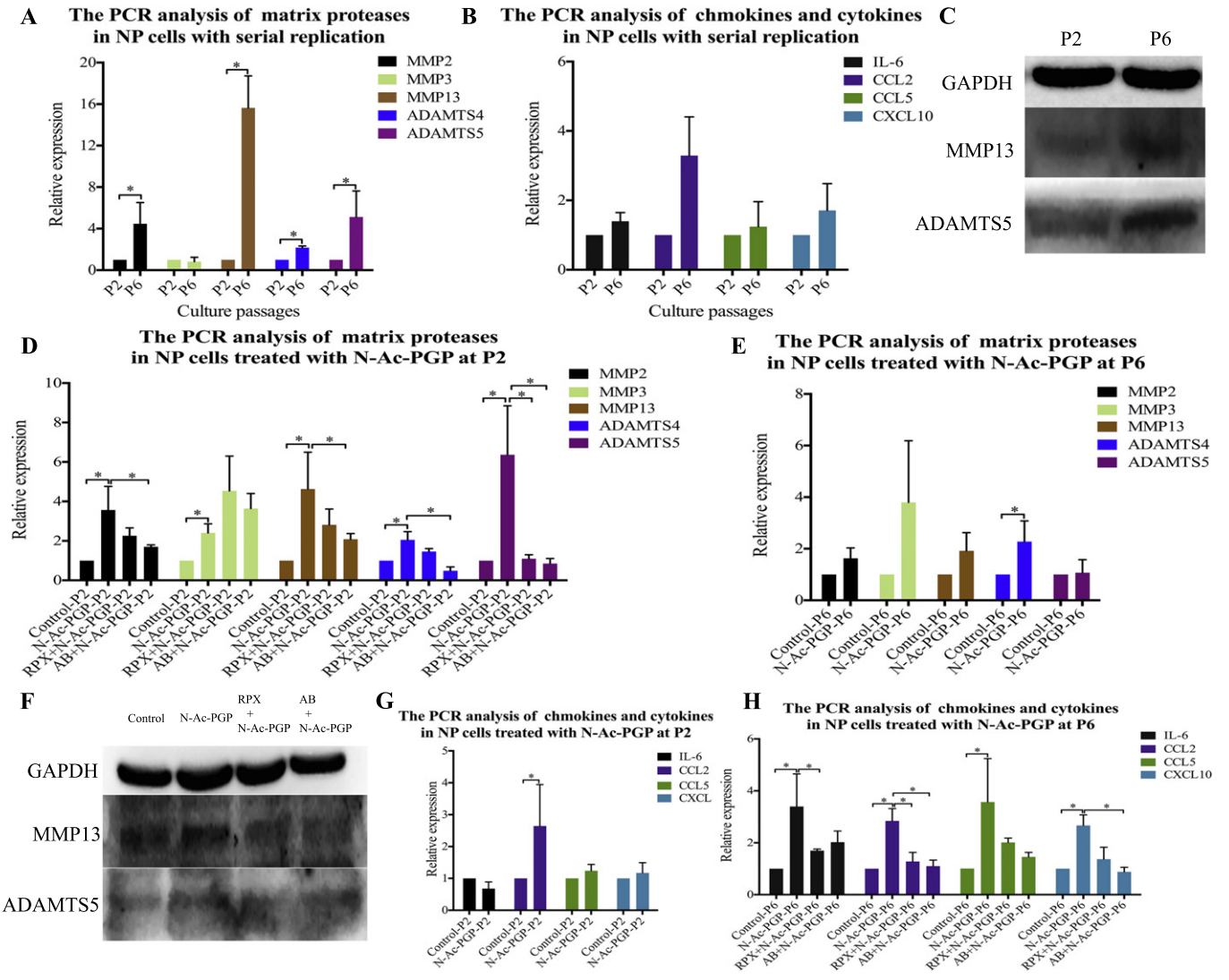

Fig. 4. N-acetylated proline-glycine-proline (N-Ac-PGP) induced the expression of matrix catabolic genes and inflammatory genes in nucleus pulposus (NP) cells. (A, B) The quantitative PCR analysis of matrix degradation enzymes and inflammatory cytokines and chemokines in untreated NP cells at different passages. (C) The western blot analysis of MMP13 and ADAMTS5 in untreated NP cells at different passages. (D, E) The quantitative PCR analysis of matrix degradation enzymes in N-Ac-PGP-treated NP cells at passage 2 (P2) or P6. (F) The western blot analysis of MMP13 and ADAMTS5 in N-Ac-PGP-treated NP cells at P2. (G, H) The quantitative PCR analysis of inflammatory cytokines in N-Ac-PGP-treated NP cells at P2 or P6. The cells without N-Ac-PGP treatment served as the control. The cells were pretreated with the RPX and AB for 30 min followed by N-Ac-PGP treatment for CXCR1 inhibition. *, P value < 0.05, error bars represent standard error. Abbreviations: RPX, Reparixin; AB, AB89251. MMP, matrix metalloproteinase; ADAMTS, a disintegrin and metalloproteinase with thrombospondin motifs.

between matrikines and cell senescence. These findings establish the regulatory functions of N-Ac-PGP in NP cell senescence, suggesting that N-Ac-PGP is an extrinsic stimulus of disc cell senescence in the harsh environment of degenerative discs. Moreover, approaches that can reduce the levels of N-Ac-PGP in IVD are expected to retard disc cell senescence. Of course, such approaches may represent promising therapeutic strategies for IDD.

N-Ac-PGP induced premature senescence of NP cells by binding to CXCR1. Mechanistically, it enhanced DNA damage and ROS accumulation in NP cells via CXCR1, without affecting the telomerase activity of NP cells. Consequently, the DNA damage response and the oxidative stress response of the NP cells were activated. Both the p53-p21-Rb and p16-Rb pathways were engaged in triggering the cell-cycle arrest of NP cells. These findings indicate that DNA damage and oxidative stress are critical intrinsic triggers of the premature senescence of NP cells induced by N-Ac-PGP. Notably, enhanced DNA damage and activation of p53 and p21 have been reported to be partially ROS dependent [26]. Whether the sustained oxidative stress is more critical for the premature senescence of NP cells induced by N-Ac-PGP will be explored in future studies. The use of anti-senescence approaches to prevent or counter oxidation and DNA damage should also be evaluated in future studies as a treatment for IDD.

In addition, the mechanism controlling N-Ac-PGP-induced ROS generation was investigated using RT^2 profiler PCR array. It showed that glutathione (GSH)-related genes (Gpx1, Gpx3 and Gsr), thioredoxin (Trx)-related genes (Txnrd1 and Txnrd 2) and other antioxidant gene (Prdx6) in NP cells were significantly down-regulated by N-Ac-PGP. The GSH and Trx are two major antioxidant systems that maintain the proper intracellular redox concentration [27]. The down-regulation of these genes suggests that N-Ac-PGP induces a decline in the antioxidants of NP cells. The balance between the antioxidant systems and ROS production in NP cells is disturbed by N-Ac-PGP, causing an increase in ROS production. The roles of antioxidant systems in disc cell senescence and IDD will be investigated in further studies.

Interestingly, the premature senescence of NP cells induced by N-Ac-PGP was attenuated with continuous culture, and the pro-senescence effects of N-Ac-PGP seemed to be eliminated with increasing passages. Based on our observations, these effects appeared to be mainly caused

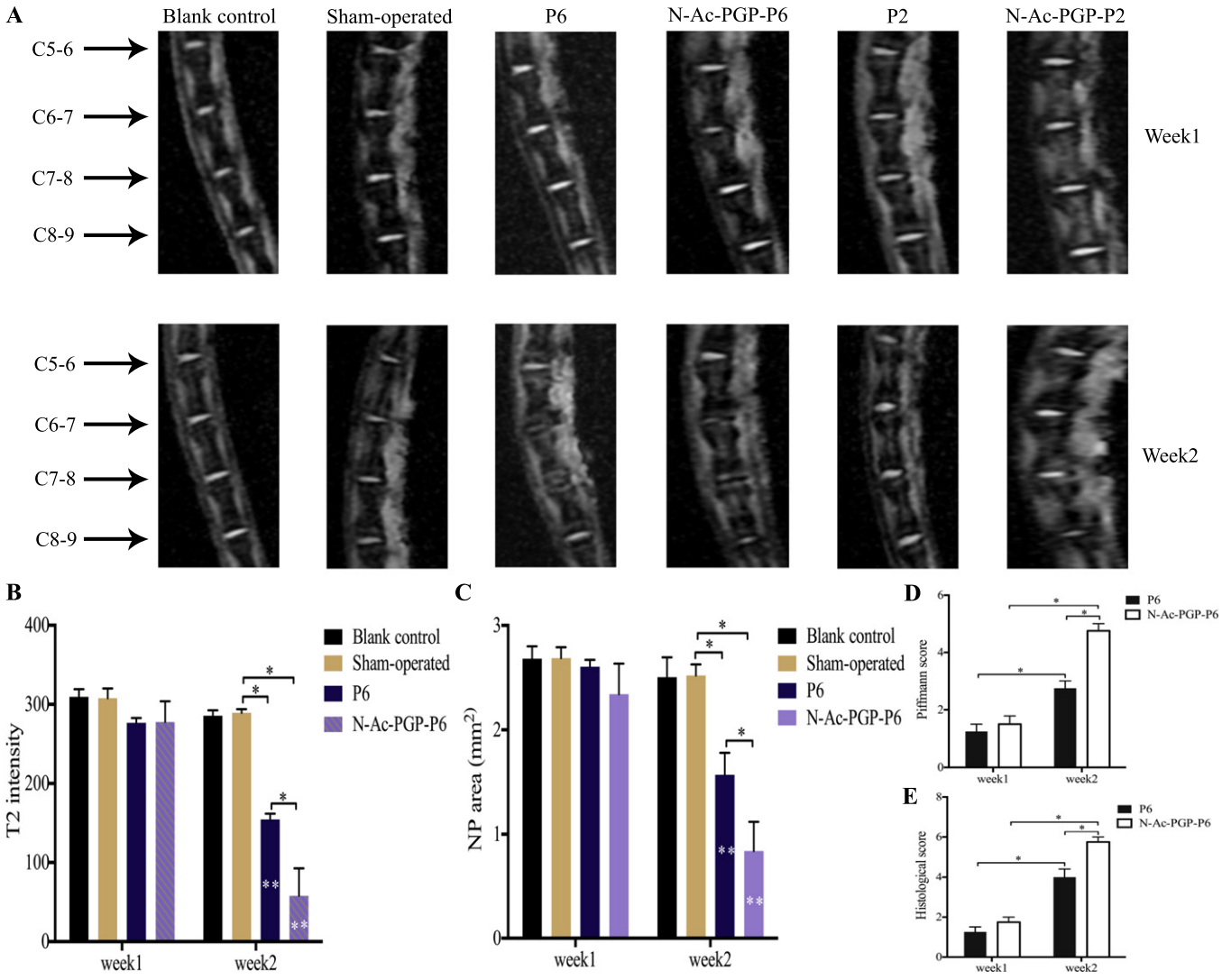

Fig. 5. The MRI characteristics and histological scores of rat caudal discs after the delivery of nucleus pulposus (NP) cells at 1 week and 2 weeks. (A) The untreated cells at passage 2 (P2) or P6 and N-acetylated proline-glycine-proline (N-Ac-PGP)-treated NP cells at P2 or P6 were delivered into C6–7 and C7–8 levels respectively. (B, C) The measurement of T2 intensity and NP area in rat caudal discs. (D) The Pfirrmann scores of rat caudal discs. (E) The histological degeneration scores of rat caudal discs. Undisturbed C5–6 and C8–9 levels served as the internal control. The rats without operation served as the blank control. Culture medium without cells was delivered into the C6–7 and C7–8 levels for the sham-operated control. *, P value < 0.05, **, P value < 0.05 compared with the blank control, error bars represent standard error.

by the spontaneous RS of NP cells with serial replication. ROS and DNA damage both accumulated spontaneously in NP cells during serial culture. Furthermore, more intrinsic triggers and extrinsic stimuli associated with cell senescence emerged at later passages, including telomere erosion and pro-inflammatory cytokines. In this context, the contribution of N-Ac-PGP to the senescence of NP cells becomes relatively decreased.

To better understand the involvement of N-Ac-PGP in the pathogenesis of IDD, the SASP of NP cells was explored. The phenotype of NP cells with RS was characterized by up-regulation of matrix proteases, cytokines and chemokines, indicating that disc cell senescence is associated with increased matrix catabolism and inflammation in degenerative discs. Importantly, N-Ac-PGP regulated the SASP of NP cells in a cell passage number-dependent manner. At early passages, N-Ac-PGP mainly activated matrix catabolic cascades in NP cells through CXCR1. In contrast, at later passages, inflammatory cascades were intensified by N-Ac-PGP through CXCR1. The N-Ac-PGP-CXCR1 complex is involved in regulating the catabolic processes and inflammatory responses of disc cells. However, the molecular mechanisms related to these passage-dependent changes should be investigated further. Notably, the NF-κB and MAPK signaling pathways have been identified as the major regulatory pathways of inflammation and matrix catabolism in degenerative discs [28]. The crosstalk between N-Ac-PGP and these molecular pathways warrants in-depth examination, and the knowledge generated would contribute to elucidating the mechanisms underlying the effects of N-Ac-PGP on the SASP of disc cells. Moreover, it might also facilitate the development of therapeutic approaches for IDD based on anti-catabolic and anti-inflammatory strategies.

With regard to the pathological significance of N-Ac-PGP in IDD, the premature senescence of disc cells induced by N-Ac-PGP led to a decrease in the number of functional and viable cells in IVDs. More seriously, N-Ac-PGP was shown to alter the phenotypic pattern of disc cells, negatively affecting the microenvironment of IVDs. The degradation of the ECM in discs is enhanced, while the increased secretion of cytokines and chemokines by senescent disc cells promotes the senescence of neighboring disc cells and increases immune cell infiltration. As a result of all three of these effects, IDD is accelerated. Our present in vivo findings provide evidence to support this idea. Intradiscal delivery of untreated cells at P6 into rat caudal IVDs caused degenerative changes in the IVDs, providing direct evidence that senescent disc cells accelerate the process of IDD. Although N-Ac-PGP induced

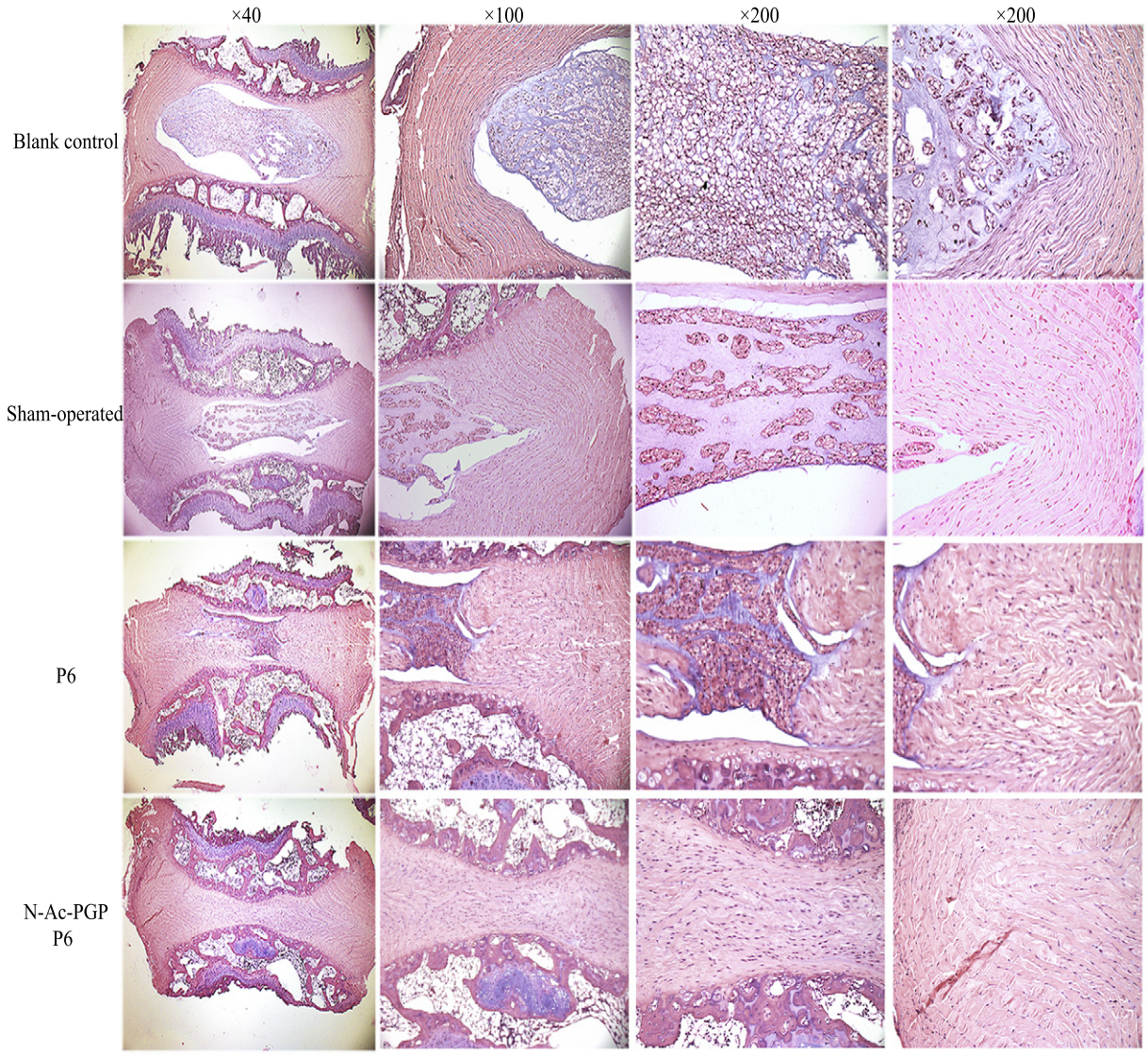

Fig. 6. Hematoxylin and eosin (H&E)-stained sections of rat caudal discs, 2 weeks after the delivery of untreated nucleus pulposus (NP) cells at passage 6 (P6) or N-acetylated proline-glycine-proline (N-Ac-PGP)-treated NP cells at P6. The discs without operation served as the blank control. The discs delivered with culture medium without cells served as the sham-operated control. ×40: 40 times magnification; ×100: 100 times magnification; ×200: 200 times magnification.

premature senescence of NP cells and enhanced the catabolic phenotype of these cells at early passages, N-Ac-PGP-treated cells at P2 did not induce IDD within two weeks. However, N-Ac-PGP-treated cells at P6 caused more severe degenerative changes than untreated cells at P6 within two weeks of implantation. These results suggest that the detrimental effects of senescent disc cells on IVD depend on the total number of senescent cells. When the number of senescent disc cells in the IVD accumulates beyond a certain threshold, they dramatically disturb the functional and structural maintenance of the IVD. This detrimental effect of senescent NP cells is reinforced by N-Ac-PGP treatment. In summary, this in vivo evidence suggests that N-Ac-PGP plays critical roles in the pathogenesis of IDD further.

There are several limitations associated with our findings. One limitation is that we used in vitro-cultured rat NP cells to investigate the roles of N-Ac-PGP in the senescence, oxidative stress and SASP of disc cells. Further studies based on human disc cells as well as in vivo evidence will be required to confirm our findings. Another limitation is that the effects of senescent NP cells on disc degeneration were evaluated using caudal IVDs of skeletally immature rats. Considering that the biochemical and biophysical properties of rat caudal discs are slightly different from human lumber discs, the results should be verified using lumber discs of skeletally mature animals to confirm the cause-effect relationship between cell senescence and IDD.

5. Conclusions

N-Ac-PGP is a potent pro-senescence matrikine in the microenvironment of IVDs. It binds to CXCR1 to induce premature senescence of NP cells through the DNA damage pathway and the ROS-dependent pathway. Furthermore, N-Ac-PGP decreases antioxidants and augments oxidative stress in NP cells. It also reinforces the inflammatory and catabolic cascades in NP cells through CXCR1, increasing the detrimental effects of senescent NP cells on the homeostasis of IVDs. Therefore, N-Ac-PGP appears to be a new therapeutic target for disc cell senescence and IDD.

Supplementary data to this article can be found online at http://dx.doi.org/10.1016/j.bbadis.2016.10.011.

Transparency document

The Transparency document associated with this article can be found in the online version.

Acknowledgements

The authors indicate no potential conflicts of interest. We thank American Journal Experts for their editing service. This study was supported by the National Natural Science Foundation of China (No. 81572186; No. 81271982; No. 81472076; No. 81272028; No. 81472131).

References

[1] S. Roberts, E.H. Evans, D. Kletsas, D.C. Jaffray, S.M. Eisenstein, Senescence in human intervertebral discs, Eur. Spine J. 15 (Suppl. 3) (2006) S312–S316.
[2] H.E. Gruber, J.A. Ingram, D.E. Davis, E.N. Hanley Jr., Increased cell senescence is associated with decreased cell proliferation in vivo in the degenerating human annulus, Spine J. 9 (2009) 210–215.
[3] A. Dimozi, E. Mavrogonatou, A. Sklirou, D. Kletsas, Oxidative stress inhibits the proliferation, induces premature senescence and promotes a catabolic phenotype in human nucleus pulposus intervertebral disc cells, Eur. Cells Mater. 30 (2015) 89–102 (discussion 103).
[4] Q.J. Xing, Q.Q. Liang, Q. Bian, D.F. Ding, X.J. Cui, Q. Shi, Y.J. Wang, Leg amputation accelerates senescence of rat lumbar intervertebral discs, Spine 35 (2010) E1253–E1261.
[5] D. Purmessur, B.A. Walter, P.J. Roughley, D.M. Laudier, A.C. Hecht, J. Iatridis, A role for TNFalpha in intervertebral disc degeneration: a non-recoverable catabolic shift, Biochem. Biophys. Res. Commun. 433 (2013) 151–156.
[6] C.L. Le Maitre, A.J. Freemont, J.A. Hoyland, Accelerated cellular senescence in degenerate intervertebral discs: a possible role in the pathogenesis of intervertebral disc degeneration, Arthritis Res. Ther. 9 (2007) R45.
[7] D.Z. Markova, C.K. Kepler, S. Addya, H.B. Murray, A.R. Vaccaro, I.M. Shapiro, D.G. Anderson, T.J. Albert, M.V. Risbud, An organ culture system to model early degenerative changes of the intervertebral disc II: profiling global gene expression changes, Arthritis Res. Ther. 15 (2013) R121.
[8] M.V. Risbud, I.M. Shapiro, Role of cytokines in intervertebral disc degeneration: pain and disc content, Nat. Rev. Rheumatol. 10 (2014) 44–56.
[9] F. Wang, F. Cai, R. Shi, X.H. Wang, X.T. Wu, Aging and age related stresses: a senescence mechanism of intervertebral disc degeneration, Osteoarthr. Cartil. 24 (2016) 398–408.
[10] S. Akthar, D.F. Patel, R.C. Beale, T. Peiro, X. Xu, A. Gaggar, P.L. Jackson, J.E. Blalock, C.M. Lloyd, R.J. Snelgrove, Matrikines are key regulators in modulating the amplitude of lung inflammation in acute pulmonary infection, Nat. Commun. 6 (2015) 8423.
[11] C.S. Hahn, D.W. Scott, X. Xu, M.A. Roda, G.A. Payne, J.M. Wells, L. Viera, C.J. Winstead, P. Bratcher, R.W. Sparidans, F.A. Redegeld, P.L. Jackson, G. Folkerts, J.E. Blalock, R.P. Patel, A. Gaggar, The matrikine N-alpha-PGP couples extracellular matrix fragmentation to endothelial permeability, Sci. Adv. 1 (2015).
[12] A. Gaggar, P.L. Jackson, B.D. Noerager, P.J. O'Reilly, D.B. McQuaid, S.M. Rowe, J.P. Clancy, J.E. Blalock, A novel proteolytic cascade generates an extracellular matrix-derived chemoattractant in chronic neutrophilic inflammation, J. Immunol. 180 (2008) 5662–5669.
[13] J.M. Wells, P.J. O'Reilly, T. Szul, D.I. Sullivan, G. Handley, C. Garrett, C.M. McNicholas, M.A. Roda, B.E. Miller, R. Tal-Singer, A. Gaggar, S.I. Rennard, P.L. Jackson, J.E. Blalock, An aberrant leukotriene A4 hydrolase-proline-glycine-proline pathway in the pathogenesis of chronic obstructive pulmonary disease, Am. J. Respir. Crit. Care Med. 190 (2014) 51–61.
[14] P.J. Koelink, S.A. Overbeek, S. Braber, M.E. Morgan, P.A. Henricks, M. Abdul Roda, H.W. Verspaget, S.C. Wolfkamp, A.A. te Velde, C.W. Jones, P.L. Jackson, J.E. Blalock, R.W. Sparidans, J.A. Kruijtzer, J. Garssen, G. Folkerts, A.D. Kraneveld, Collagen degradation and neutrophilic infiltration: a vicious circle in inflammatory bowel disease, Gut 63 (2014) 578–587.
[15] J.W. Hill, E.M. Nemoto, Matrix-derived inflammatory mediator N-acetyl proline-glycine-proline is neurotoxic and upregulated in brain after ischemic stroke, J. Neuroinflammation 12 (2015) 214.
[16] C. Feng, Y. Zhang, M. Yang, B. Huang, Y. Zhou, Collagen-derived N-acetylated proline-glycine-proline in intervertebral discs modulates CXCR1/2 expression and activation in cartilage endplate stem cells to induce migration and differentiation toward a pro-inflammatory phenotype, Stem Cells 33 (2015) 3558–3568.
[17] J.C. Acosta, A. O'Loghlen, A. Banito, M.V. Guijarro, A. Augert, S. Raguz, M. Fumagalli, M. Da Costa, C. Brown, N. Popov, Y. Takatsu, J. Melamed, F.d.'A. di Fagagna, D. Bernard, E. Hernando, J. Gil, Chemokine signaling via the CXCR2 receptor reinforces senescence, Cell 133 (2008) 1006–1018.
[18] H. Guo, Z. Liu, B. Xu, H. Hu, Z. Wei, Q. Liu, X. Zhang, X. Ding, Y. Wang, M. Zhao, Y. Gong, C. Shao, Chemokine receptor CXCR2 is transactivated by p53 and induces p38-mediated cellular senescence in response to DNA damage, Aging Cell 12 (2013) 1110–1121.
[19] M. Muller, Cellular senescence: molecular mechanisms, in vivo significance, and redox considerations, Antioxid. Redox Signal. 11 (2009) 59–98.
[20] C.W. Pfirrmann, A. Metzdorf, M. Zanetti, J. Hodler, N. Boos, Magnetic resonance classification of lumbar intervertebral disc degeneration, Spine 26 (2001) 1873–1878.
[21] G. Keorochana, J.S. Johnson, C.E. Taghavi, J.C. Liao, K.B. Lee, J.H. Yoo, S.S. Ngo, J.C. Wang, The effect of needle size inducing degeneration in the rat caudal disc: evaluation using radiograph, magnetic resonance imaging, histology, and immunohistochemistry, Spine J. 10 (2010) 1014–1023.
[22] A. Hiyama, D. Sakai, M.V. Risbud, M. Tanaka, F. Arai, K. Abe, J. Mochida, Enhancement of intervertebral disc cell senescence by WNT/beta-catenin signaling-induced matrix metalloproteinase expression, Arthritis Rheum. 62 (2010) 3036–3047.
[23] A. Freund, A.V. Orjalo, P.Y. Desprez, J. Campisi, Inflammatory networks during cellular senescence: causes and consequences, Trends Mol. Med. 16 (2010) 238–246.
[24] S.W. Jeong, J.S. Lee, K.W. Kim, In vitro lifespan and senescence mechanisms of human nucleus pulposus chondrocytes, Spine J. 14 (2014) 499–504.
[25] C. Feng, H. Liu, M. Yang, Y. Zhang, B. Huang, Y. Zhou, Disc cell senescence in intervertebral disc degeneration: causes and molecular pathways, Cell Cycle 15 (2016) 1674–1684.
[26] J.I. Jun, L.F. Lau, The matricellular protein CCN1 induces fibroblast senescence and restricts fibrosis in cutaneous wound healing, Nat. Cell Biol. 12 (2010) 676–685.
[27] S.F. Tadros, M. D'Souza, X. Zhu, R.D. Frisina, Gene expression changes for antioxidants pathways in the mouse cochlea: relations to age-related hearing deficits, PLoS One 9 (2014), e90279.
[28] K. Wuertz, N. Vo, D. Kletsas, N. Boos, Inflammatory and catabolic signalling in intervertebral discs: the roles of NF-kappaB and MAP kinases, Eur. Cells Mater. 23 (2012) 103–119 (discussion 119-120).